

Multi-GNSS Real-time Precise Point Positioning: GPS, GLONASS, BeiDou, and Galileo

Xingxing Li, Maorong Ge, Mathias Fritsche, Yang Liu, Zhiguo
Deng, Jens Wickert, and Harald Schuh

*The German Research Centre for Geosciences (GFZ)
Telegrafenberg, Potsdam, Germany. lixin@gfz-potsdam.de*

Content

- 1 Multi-GNSS status**
- 2 Multi-GNSS data processing**
- 3 Multi-GNSS orbit and clock**
- 4 Multi-GNSS real-time PPP**
- 5 Discussions**

1 Current multi-GNSS status

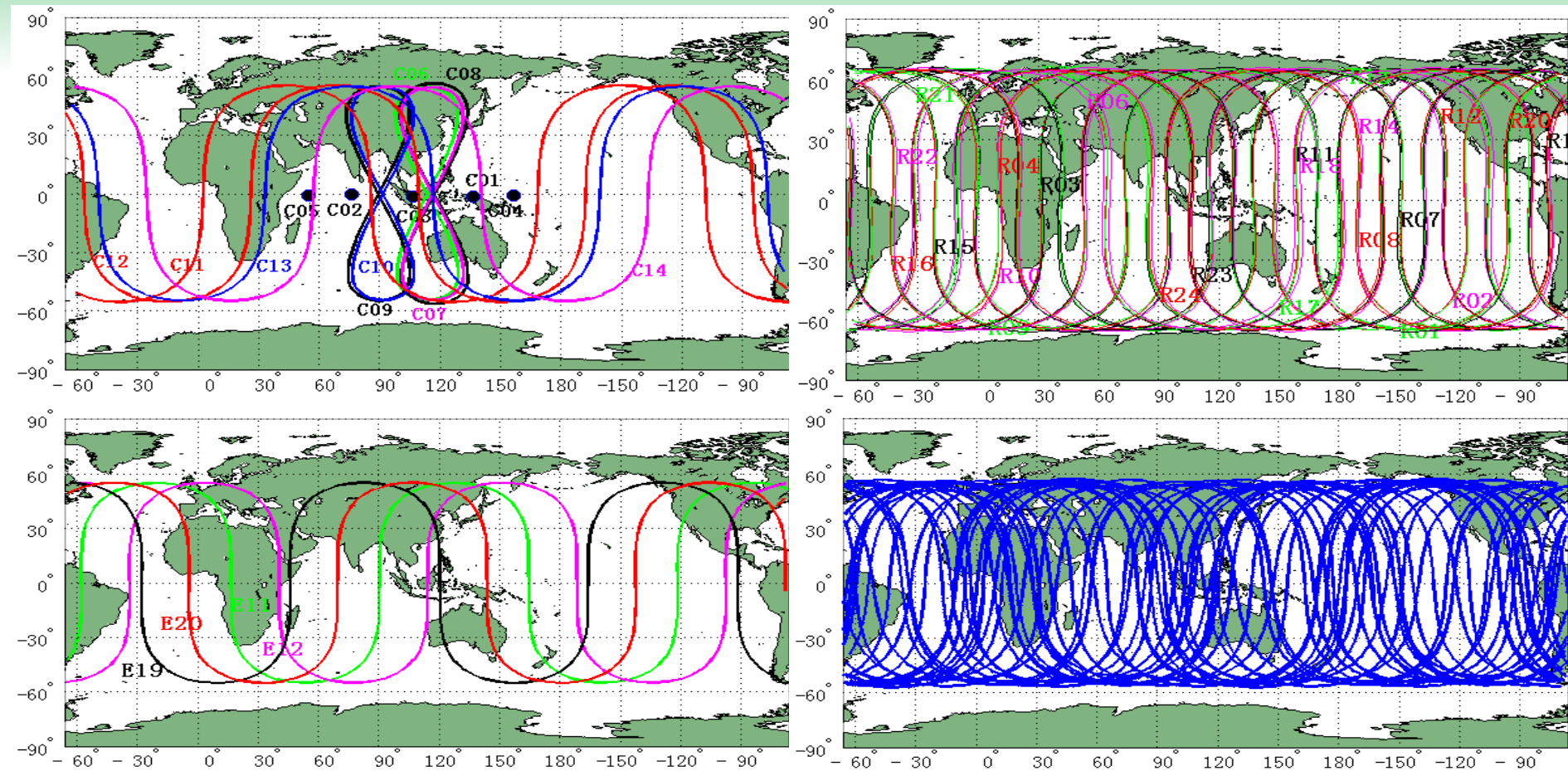


Figure 1. Ground tracks of four satellite navigation systems: BeiDou (14), Galileo (8+), GLONASS (24) and GPS (32).

1 Current multi-GNSS status

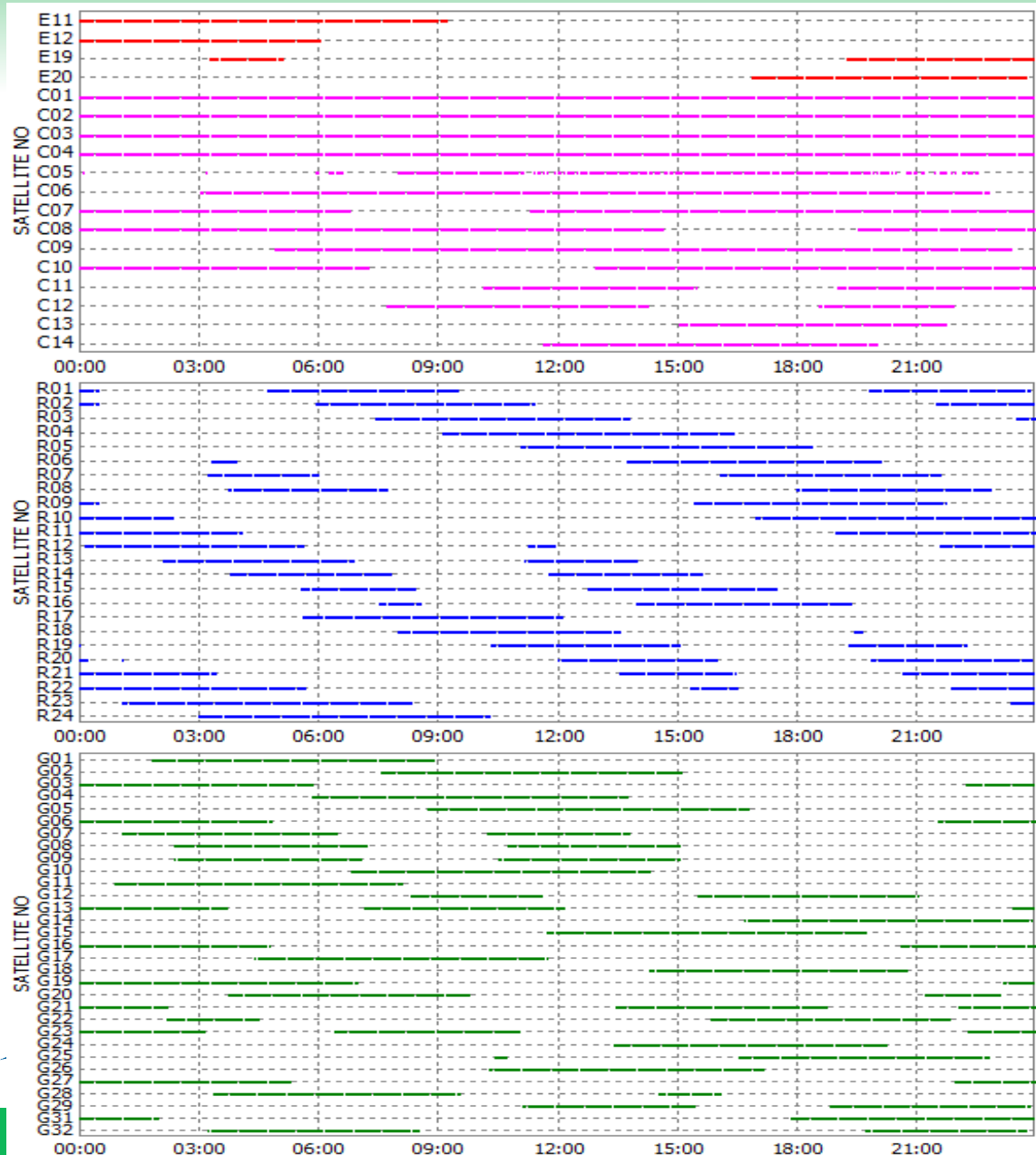


Figure 2. Satellite visibility of Galileo, BeiDou, GLONASS and GPS at the four-system station GMSD (Japan) on September 3, 2013 .

Li et al (2015), Precise positioning with current multi-constellation Global Navigation Satellite Systems: GPS, GLONASS, Galileo and BeiDou. Sci Rep., 5, 8328.

1 Current multi-GNSS status

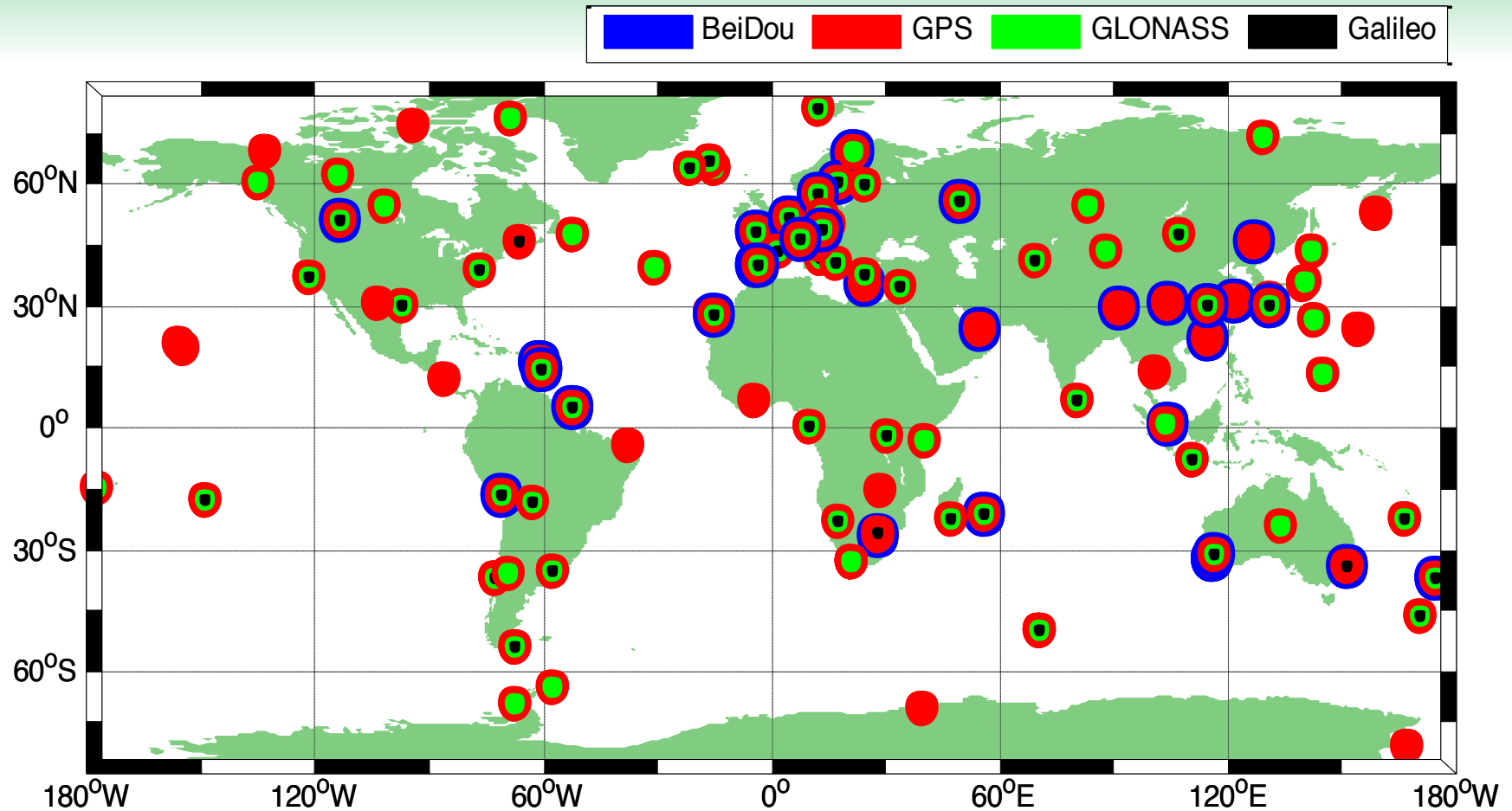


Figure 3. Distribution of MGEX stations and their supported constellations (as of 2014, almost 90 stations); some IGS stations (the red circles, GPS-only) are also included.

1 Current multi-GNSS status

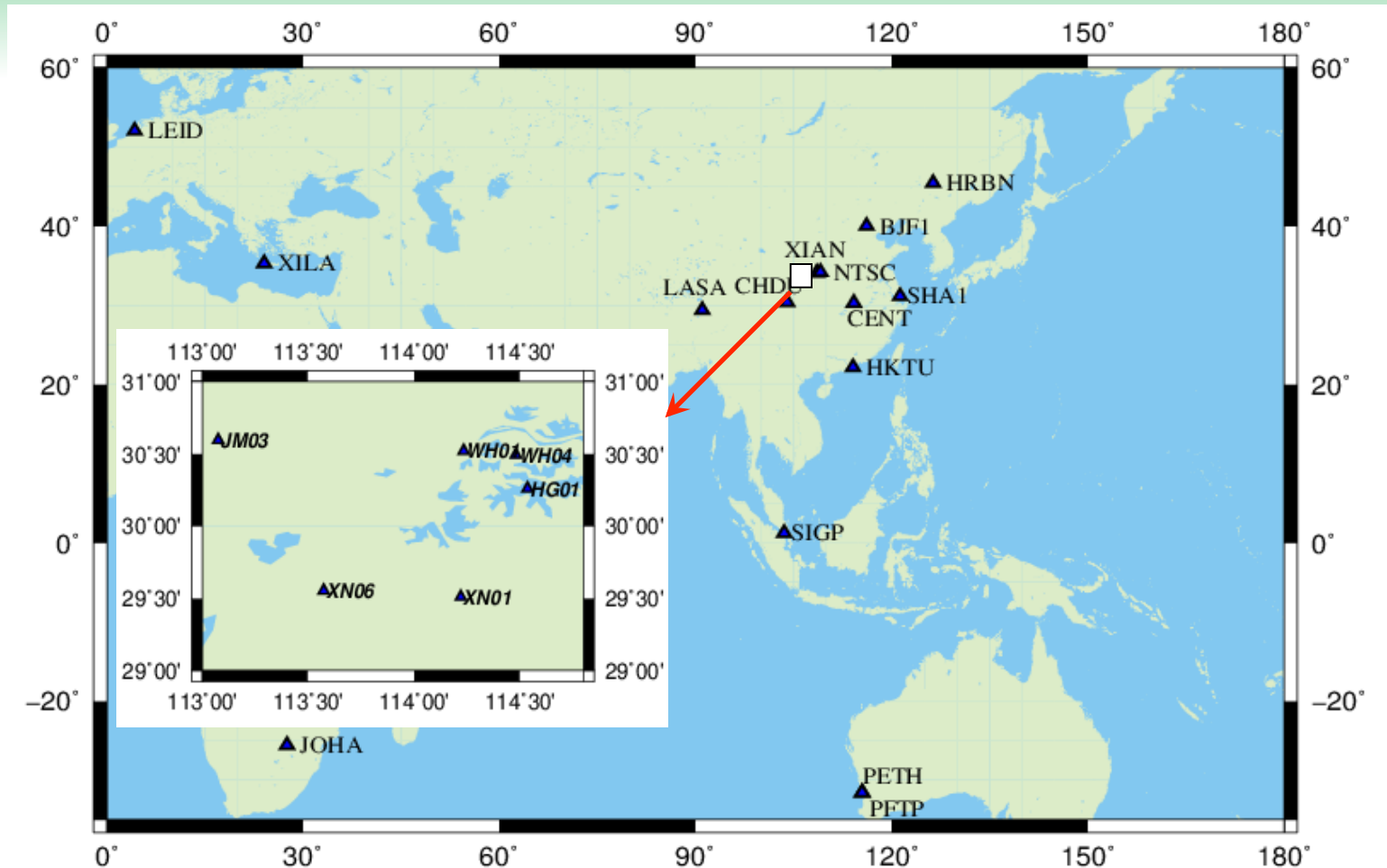


Figure 4. BETN (WHU) and a local CORS network equipped with GPS+BeiDou capable dual-system receivers. The small map indicates the local CORS network and the large one is for BETN.

2 Multi-GNSS data processing

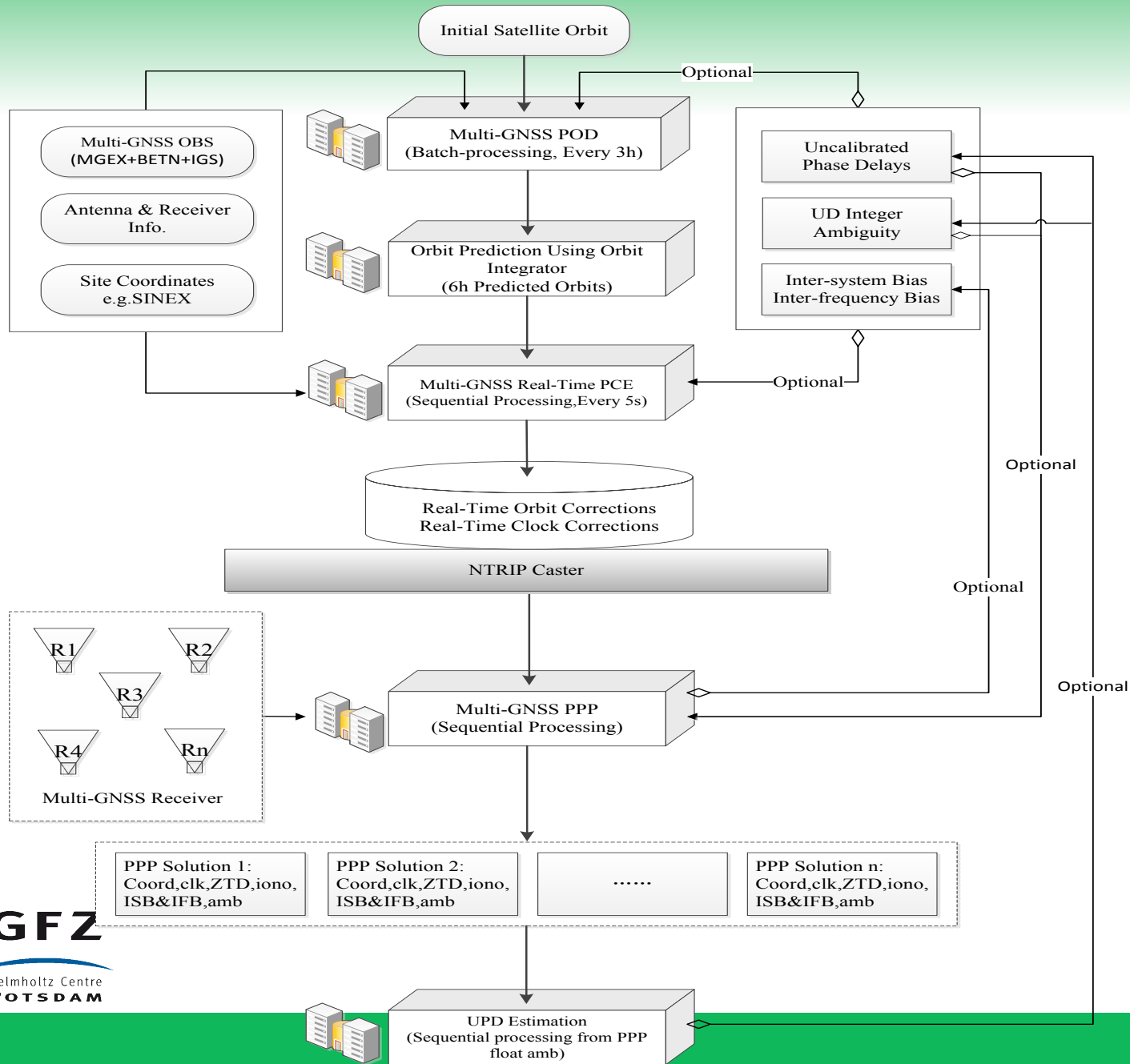


Figure 5. The structure of the prototype multi-GNSS real-time PPP service system at GFZ.

2 Multi-GNSS data processing

Item	Models
Satellites	BeiDou+Galileo+GLONASS+GPS; about 74 satellites
Procedure	Integrated processing, all the observations from different GNSS in one common parameter adjustment procedure
Estimator	LSQ in batch mode for POD; LSQ in sequential mode for PCE & PPP
Observations	Undifferenced phase and code observations
Combination mode	Ionosphere-free combination for POD/PCE network solution; raw observations on individual frequencies for PPP
Signal selection	GPS: L1/L2; GLONASS: L1/L2; BeiDou: B1/B2; Galileo: E1/E5a
Tracking data	IGS+MGEX+BETN (about 120 stations) for POD and PCE; Local CORS and some MGEX stations are selected for PPP
Sampling rate	30s
Elevation cutoff	7°
Observation weight	Elevation dependent weight
Phase-windup effect	Corrected
Earth rotation parameter	Estimated with tight constraint (He et al., 2013b)
Tropospheric delay	Initial model + random-walk process
Ionospheric delay	Eliminated by IF combination in POD and PCE; estimated as parameters in PPP
Receiver clock	Estimated, white noise
ISB and IFB	Estimated as constant with zero mean conditions in post; introduced as known values in RT
Station displacement	Solid Earth tide, pole tide, ocean tide loading, IERS Convention 2003 (McCarthy and Petit, 2003)
Satellite antenna phase center	Corrected using MGEX and IGS values
Receiver antenna phase center	Corrected using GPS values
Terrestrial frame	ITRF2008 (Altamimi et al., 2011)
Satellite orbit	Estimated in POD; Fixed in PCE&PPP using the products from POD
GFZ Satellite clock	Estimated in POD and PCE, white noise; Fixed in PPP using the products from PCE
Station coordinate	Fixed (or tightly constrained) in POD and PCE; Estimated in epoch-wise kinematic for PPP
Phase ambiguities	Constant for each arc; DD AR for network solution, undifferenced AR if UPD

Table 1. Multi-GNSS data processing strategy, observation models and estimated parameters for POD, PCE, and PPP

Li et al (2015), Accuracy and reliability of multi-GNSS real-time precise positioning: GPS, GLONASS, BeiDou, and Galileo. *J. Geod.*, 2015, 89(6): 607-635.

2 Multi-GNSS data processing

Item	Models
Orbit arc	3-day solution
Geopotential	EGM96 model (12×12)
Tide	Solid Earth tide, pole tide, ocean tide IERS Conventions 2003
M-body gravity	Sun, Moon and all planets (JPL DE405)
Solar Radiation Pressure	Bern five parameters with no initial value
Relativistic Effect	Applied
Velocity breaks	Every other 12 hours
Attitude model	Nominal attitude for GPS/GLONASS/Galileo; Nominal attitude with yaw maneuver for MEO and IGSO satellites of BeiDou; Yaw-fixed attitude mode used for GEO satellites of BeiDou

Table 2. Dynamical models involved for multi-GNSS POD.

3 Multi-GNSS orbit and clock

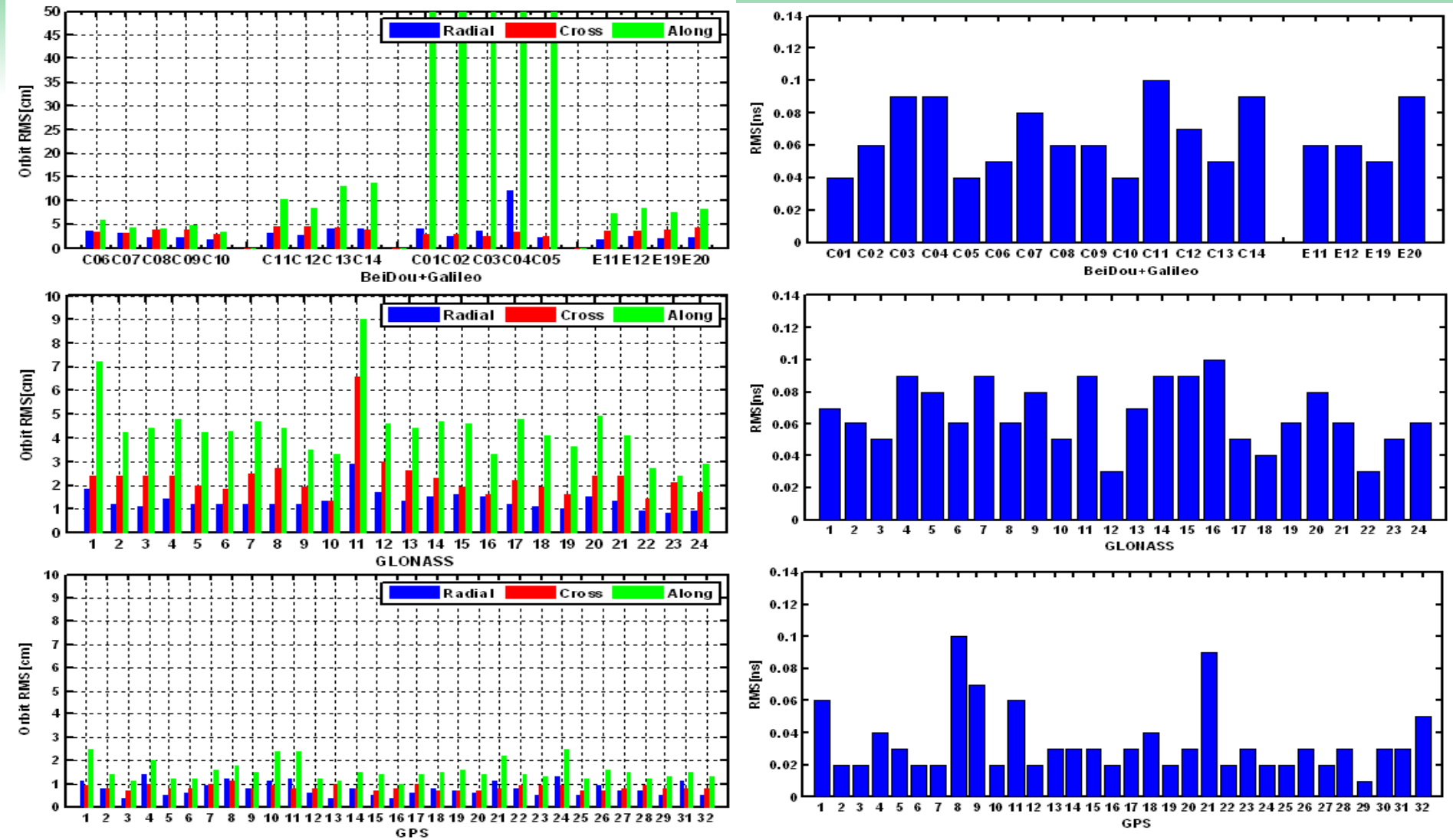


Figure 6. Averaged RMS values of 48 h orbit and clock overlap differences in radial, cross, and along directions .

3 Real-time orbit and clock

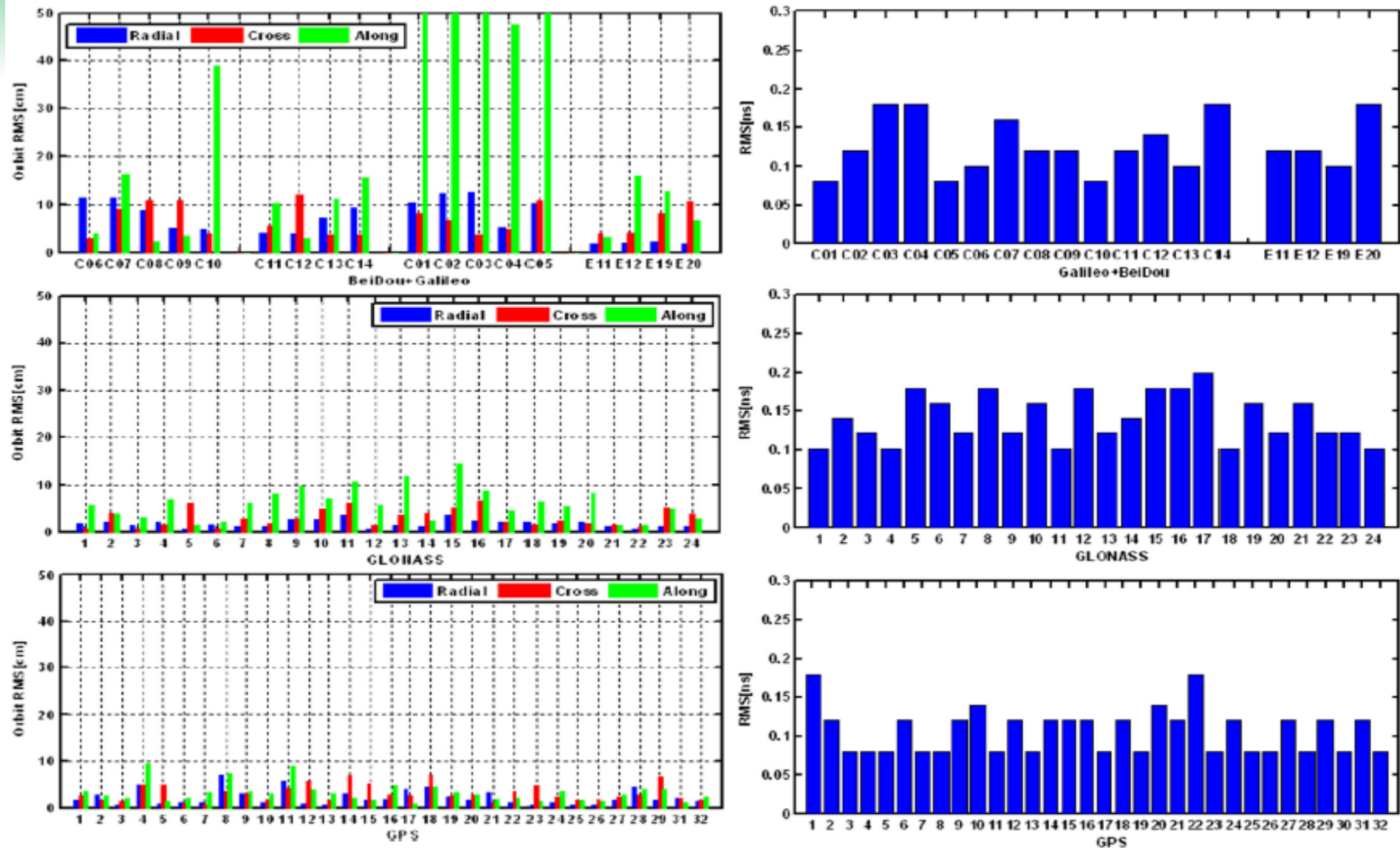


Figure 7. Averaged RMS values of orbit and clock differences between the real-time and post-processed solutions

3 Real-time orbit and clock

Satellite	R(cm)	C(cm)	A(cm)	3D(cm)
BeiDou IGSO	8.3	7.5	13.0	17.1
BeiDou MEO	6.3	6.2	12.0	14.9
BeiDou GEO	10.1	6.8	92.7	93.4
Galileo	2.9	6.8	9.8	12.2
GLONASS	2.2	3.1	5.9	7.0
GPS	1.8	3.0	3.2	4.7

Table 3. The averaged RMS values of predicted orbit differences in along- (A), cross-track (C) and radial (R) components.

4 Multi-GNSS real-time PPP

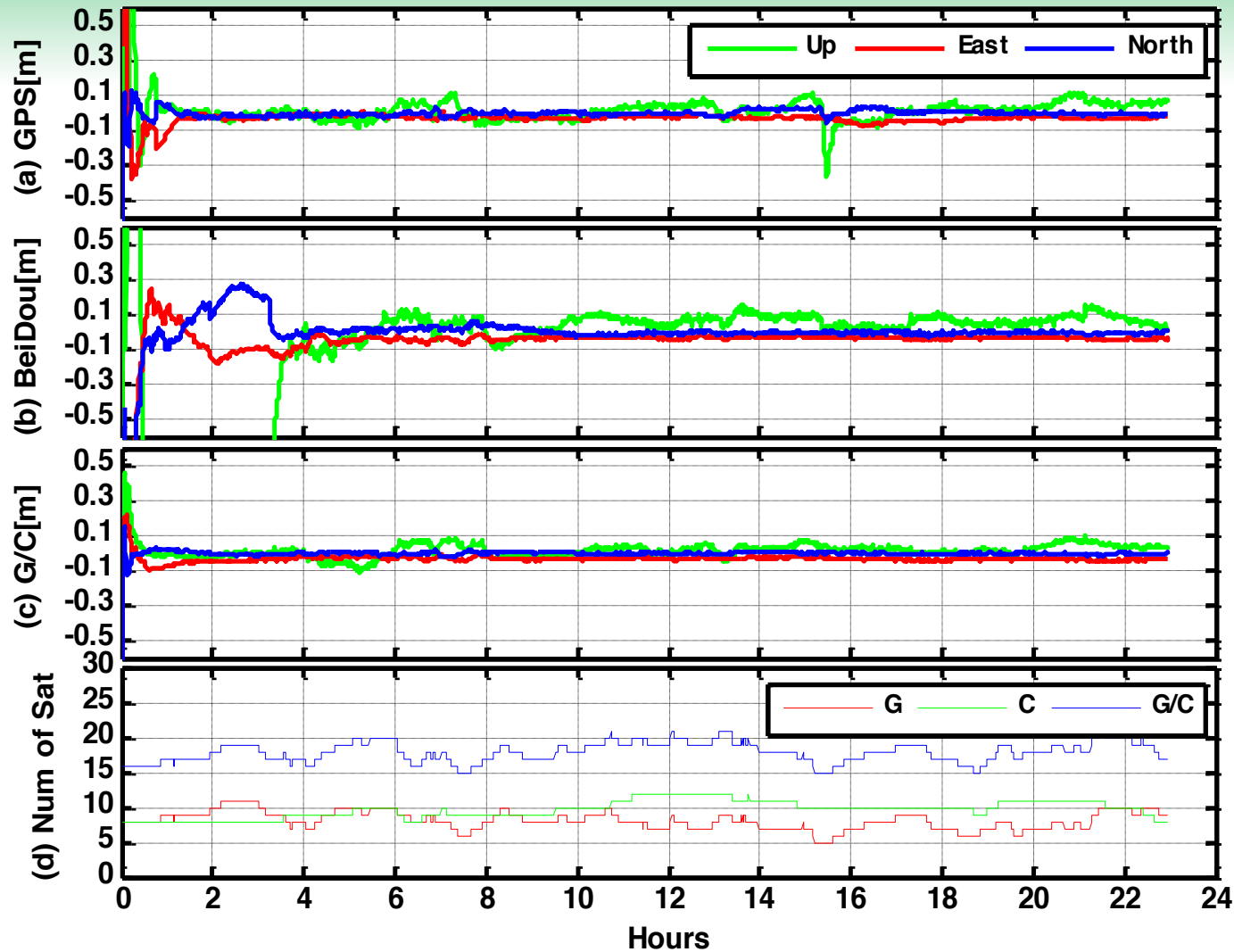


Figure 8. Comparisons of GPS, BeiDou and GPS/BeiDou kinematic PPP solutions at station CENT.

4 Multi-GNSS real-time PPP

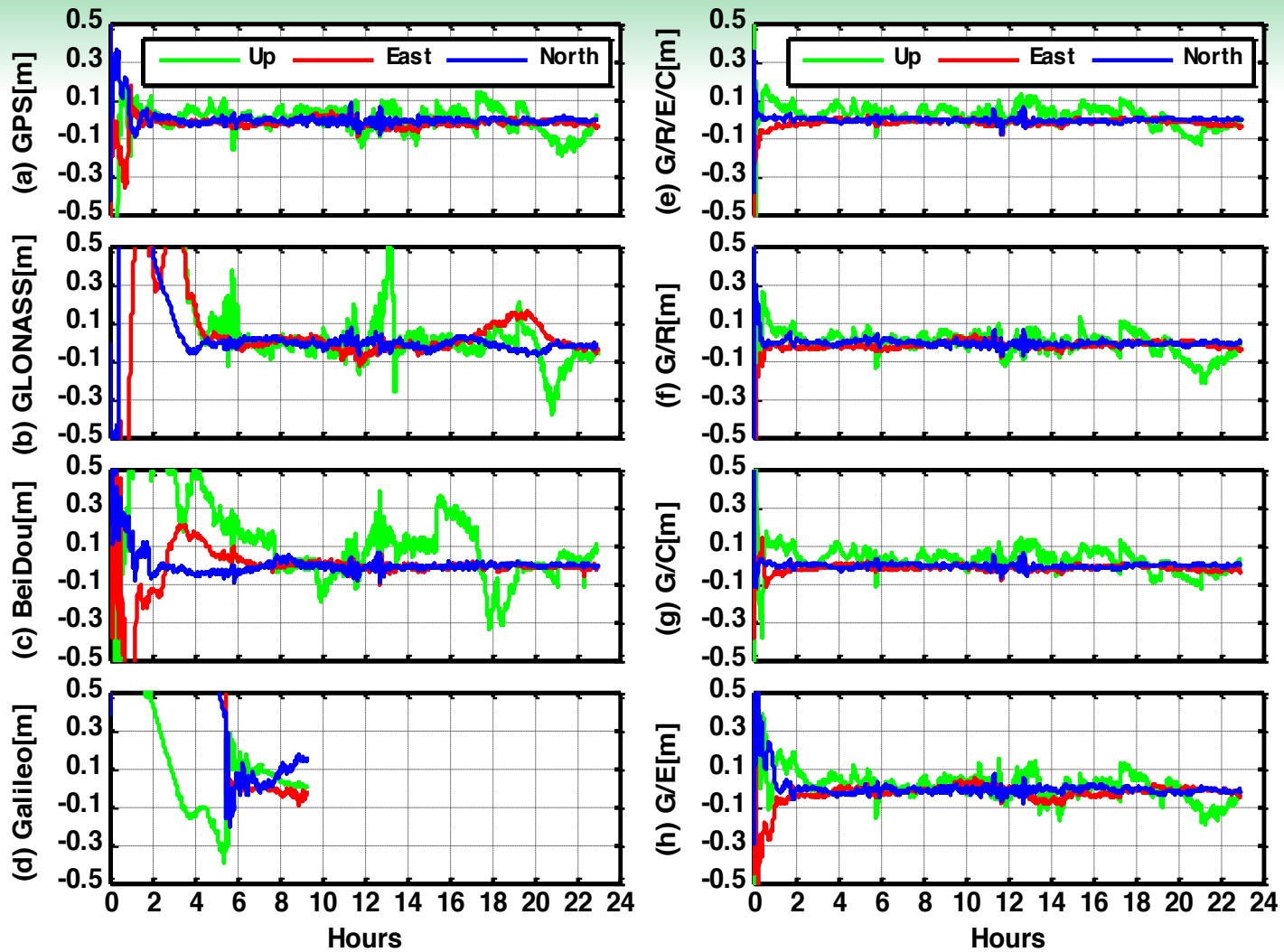


Figure 9. Kinematic PPP solutions of single-system, dual-system and four-system modes at station GMSD.

4 Multi-GNSS real-time PPP

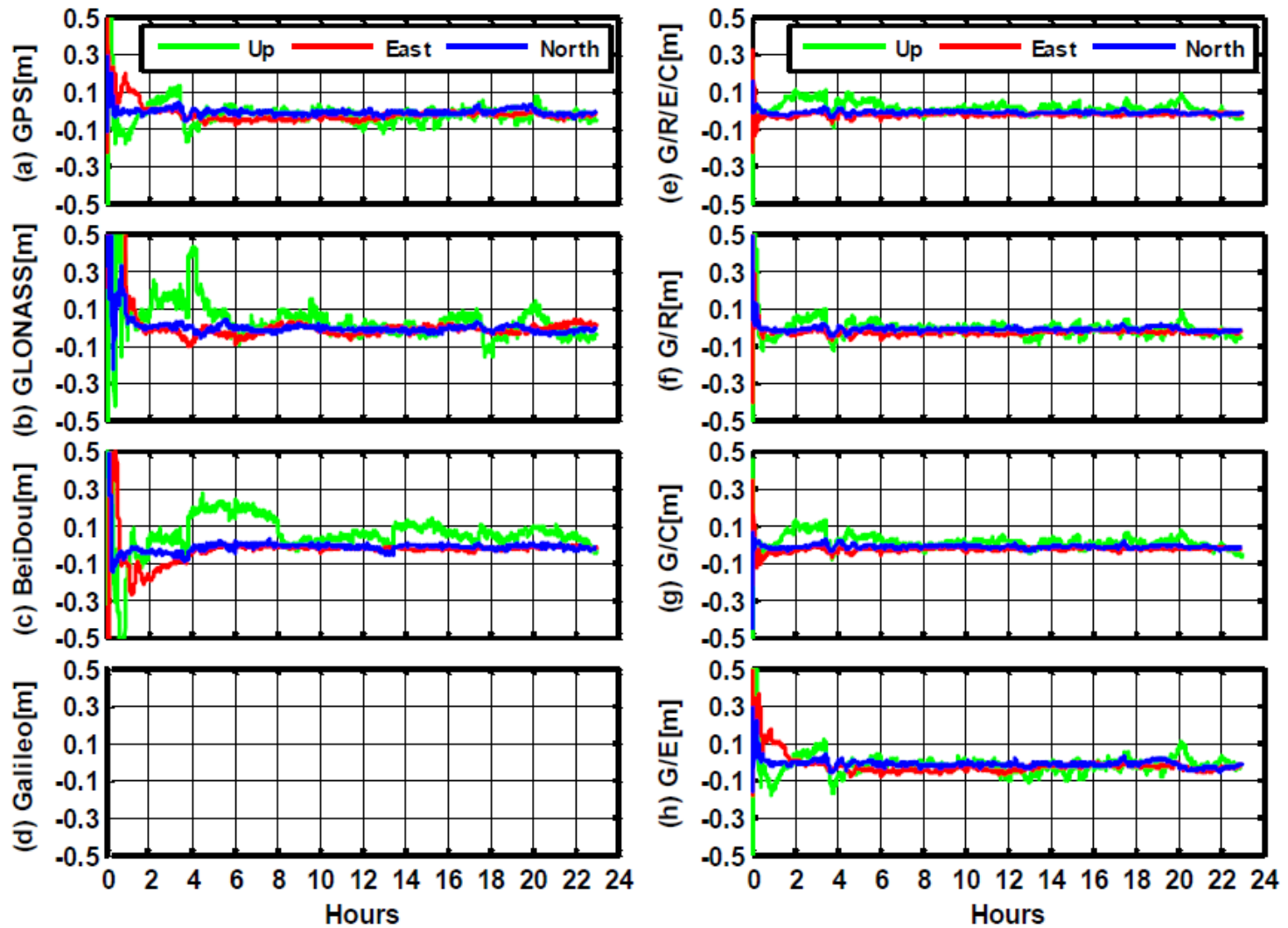


Figure 10. Kinematic PPP solutions of single-system, dual-system and four-system modes at station CUT0.

4 Multi-GNSS real-time PPP

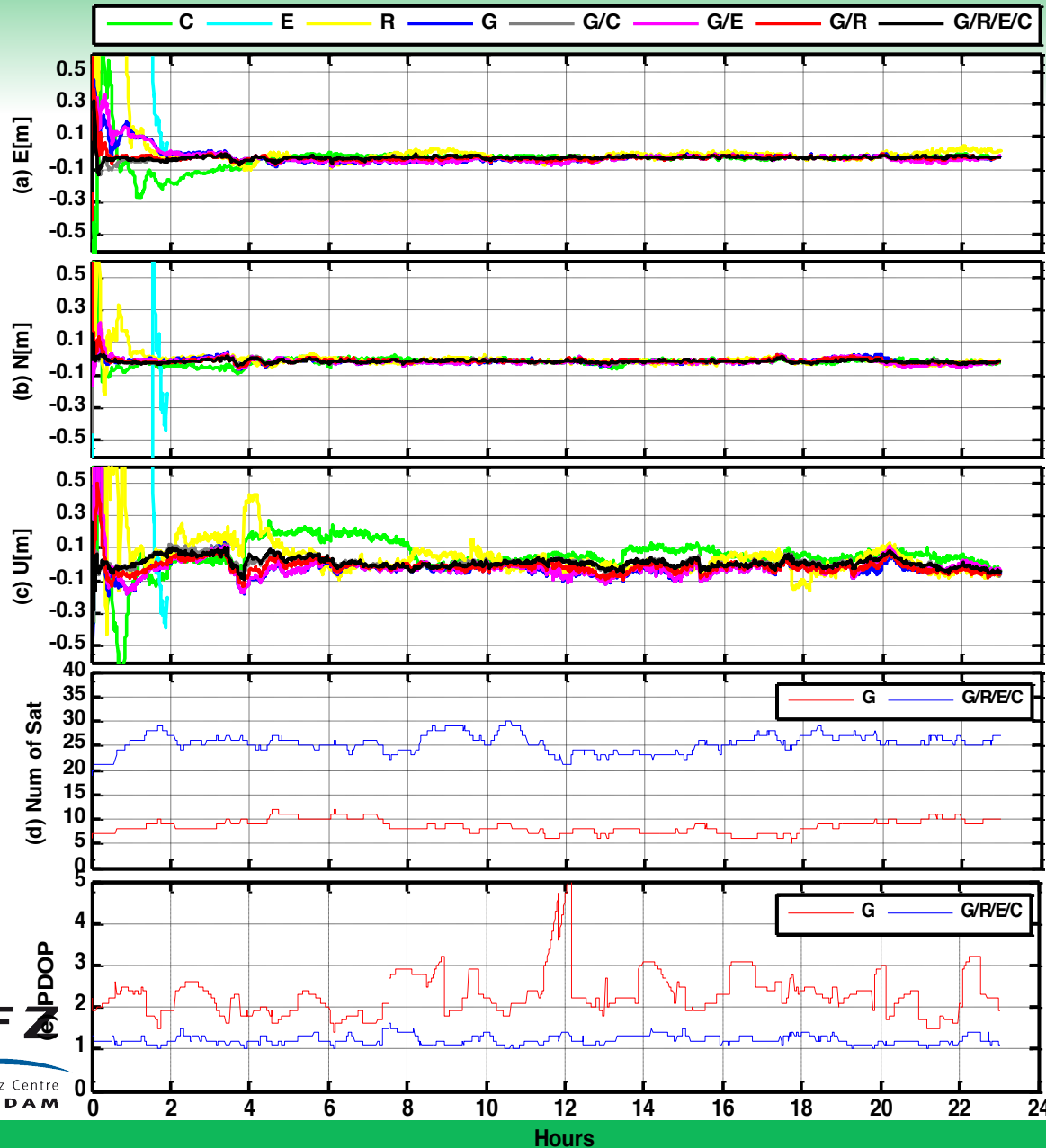


Figure 11. Comparisons of PPP results from different single-system and combined solutions in the east, north and up components, respectively at station CUT0.

4 Multi-GNSS real-time PPP

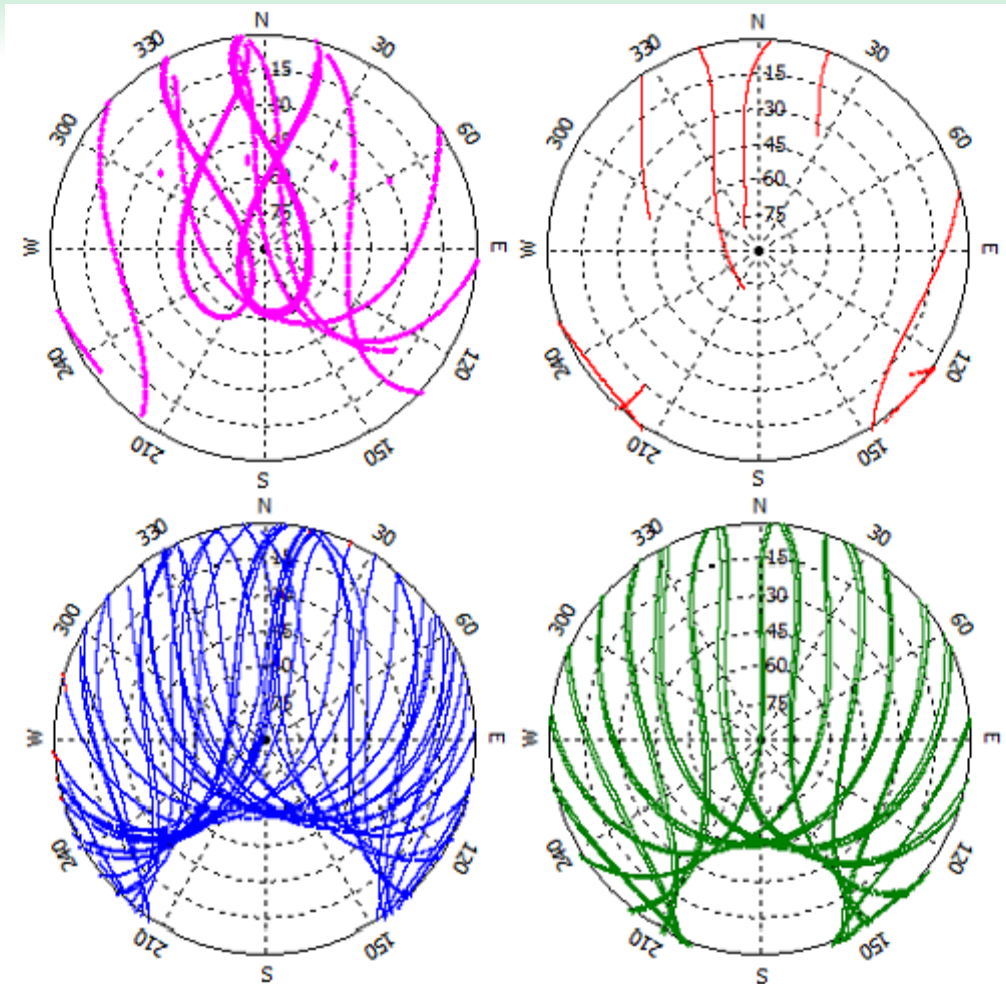


Figure 12. Sky plots (azimuth vs elevation) of the four GNSS (BeiDou in pink, Galileo in red, GPS in blue and GLONASS in green) for CUT0.

4 Multi-GNSS real-time PPP

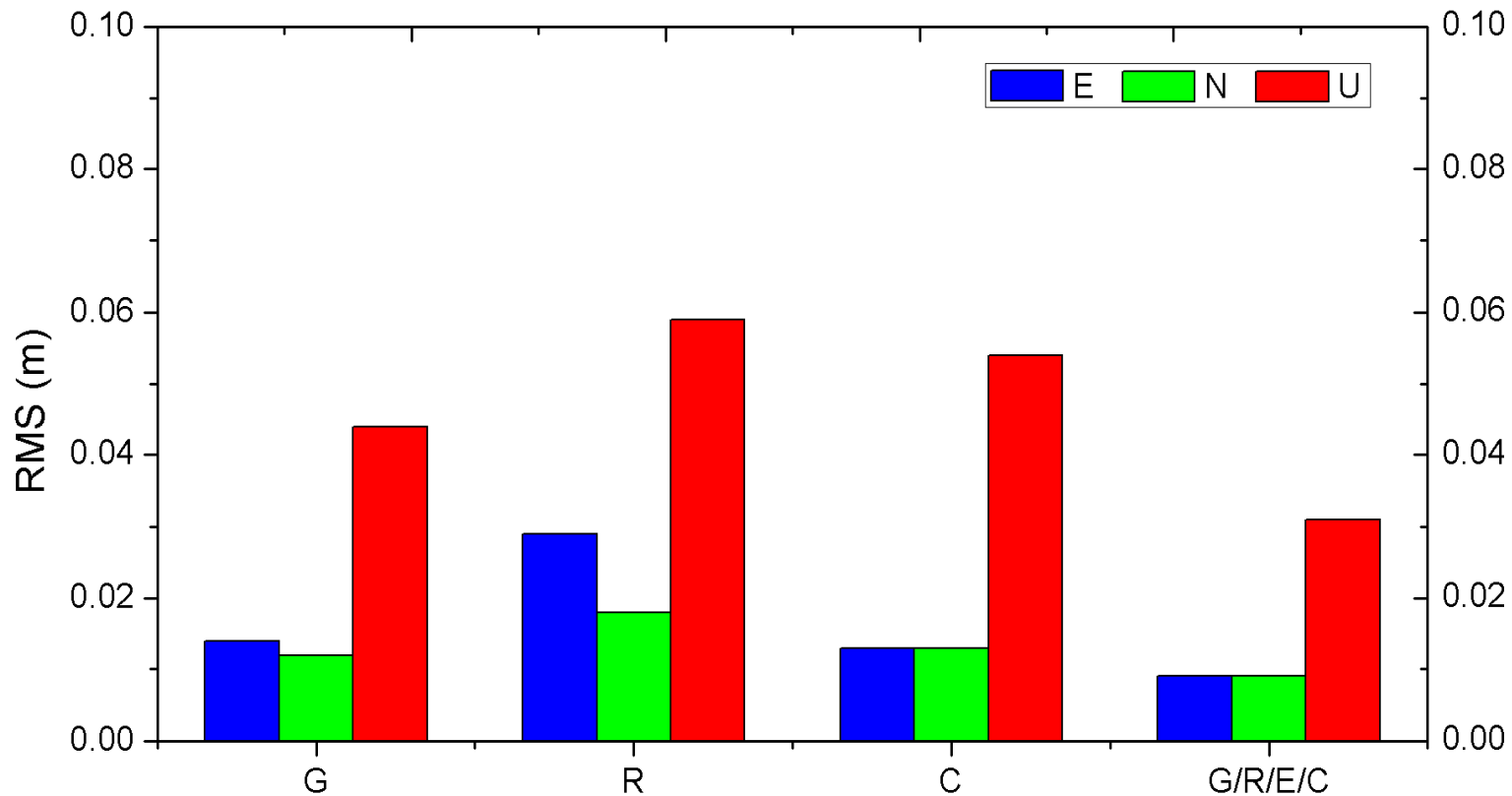


Figure 13. The averaged RMS values of all the stations for kinematic PPP solutions in north, east and up components.

4 Multi-GNSS real-time PPP

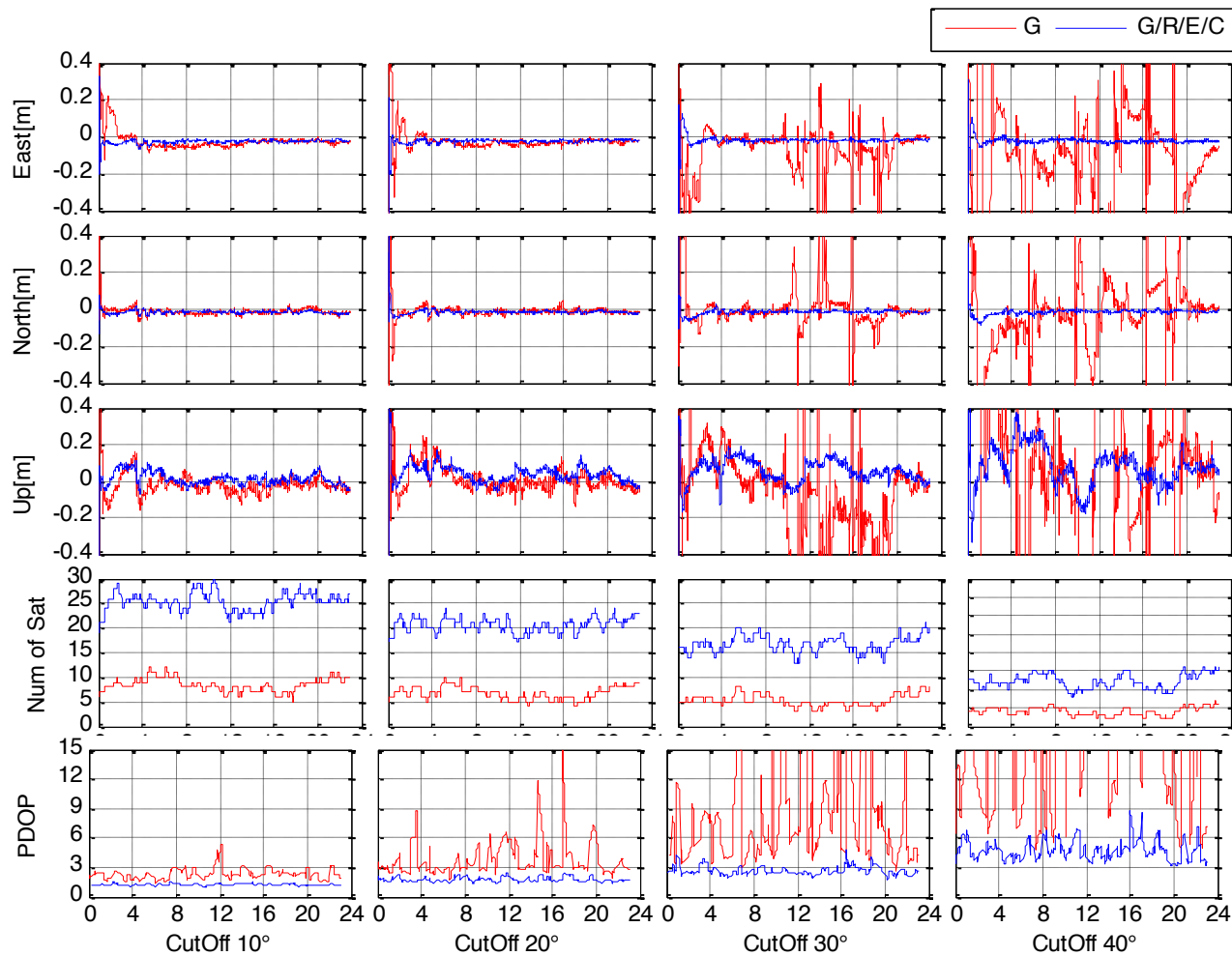


Figure 14. Comparisons of PPP results in single- and multi-system modes under different elevation cutoffs (from 10° to 40°) at station CUT0.

4 Multi-GNSS real-time PPP

Station	GPS (%)				G/R/E/C (%)			
	10°	20°	30°	40°	10°	20°	30°	40°
CENT	100.0	99.6	89.2	41.5	100.0	100.0	100.0	100.0
CHDU	99.7	98.3	84.7	46.0	100.0	100.0	100.0	100.0
SIGP	94.8	93.7	72.1	39.2	100.0	100.0	99.9	99.5
CUT0	96.8	95.0	89.3	57.6	100.0	100.0	100.0	100.0
GMSD	98.1	97.6	79.5	30.2	100.0	100.0	100.0	99.8
NNOR	99.2	93.8	78.6	37.8	100.0	100.0	100.0	100.0
ONS1	96.1	93.3	62.5	30.6	100.0	100.0	99.9	99.6

$$f_{availability} = \frac{N_{precise}}{N_{total}}$$

Table 4. The empirical availability rates (in %) for the single- and multi-GNSS under different elevation cutoffs (from 10° to 40°) .

Discussions

◆ The performance of the multi-GNSS processing will be further improved in the next years along with the launch of more satellites and the setup of more multi-GNSS stations.

◆ The Multi-GNSS will bring many benefits for Geosciences applications:

Li et al. (2015), Retrieving of atmospheric parameters from multi-GNSS in real-time: Validation with water vapor radiometer and numerical weather model. JGR.

Li et al. (2015), Retrieving high-resolution tropospheric gradients from multi-constellation GNSS observations. GRL, DOI:10.1002/2015GL063856

Lu et al. (2015), Real-time retrieval of precipitable water vapor from GPS and BeiDou observations. Journal of Geodesy, DOI:10.1007/s00190-015-0818-0

Li et al. (2015), Multi-GNSS meteorology: Real-time retrieving of atmospheric water vapor from BeiDou, Galileo, GLONASS and GPS observations. IEEE Transactions on Geoscience and Remote Sensing, DOI:10.1109/TGRS.2015.2438395

.....

Thank you !